

ASR-SYNCHRONIZED SPEAKER-ROLE DIARIZATION

Arindam Ghosh, Mark Fuhs, Bongjun Kim, Anurag Chowdhury, Monika Woszczyna

Solventum Health Information Systems, USA

ABSTRACT

Speaker-role diarization (RD), such as doctor vs. patient or lawyer vs. client, is practically often more useful than conventional speaker diarization (SD), which assigns only generic labels (speaker-1, speaker-2). The state-of-the-art end-to-end ASR+RD approach uses a single transducer that serializes word and role predictions (role at the end of a speaker’s turn), but at the cost of degraded ASR performance. To address this, we adapt a recent joint ASR+SD framework to ASR+RD by freezing the ASR transducer and training an auxiliary RD transducer in parallel to assign a role to each ASR-predicted word. For this, we first show that SD and RD are fundamentally different tasks, exhibiting different dependencies on acoustic and linguistic information. Motivated by this, we propose (1) task-specific predictor networks and (2) using higher-layer ASR encoder features as input to the RD encoder. Additionally, we replace the blank-shared RNNT loss by cross-entropy loss along the 1-best forced-alignment path to further improve performance while reducing computational and memory requirements during RD training. Experiments on a public and a private dataset of doctor–patient conversations demonstrate that our method outperforms the best baseline with relative reductions of 6.2% and 4.5% in role-based word diarization error rate (R-WDER), respectively.

Index Terms— ASR, diarization, speaker-role, transducer, RNNT loss

1. INTRODUCTION

In multi-speaker conversations like doctor-patient encounters, lawyer-client interactions, meetings, etc., ASR captures “what was spoken” while speaker diarization (SD) determines “who spoke when.” Combining the two, joint ASR + SD determines “who spoke what,” which improves the intelligibility of, otherwise lengthy and unstructured, transcripts and helps downstream natural language processing (NLP) tasks, such as summarization, information extraction, etc., with more accurate and meaningful insights.

An issue with SD is that it assigns generic labels (e.g. speaker-1, speaker-2) without any prior knowledge of their identities [4]. For real-world applications, such as summarization, identifying the *speaker-role* (doctor, patient, lawyer, client, etc.) is more valuable than knowing the actual speaker identity. Although one can utilize external speaker profiles to map the generic SD labels to actual speakers, enabling role inference, such external data is often unavailable. In these scenarios, joint ASR + speaker-role diarization (RD) that directly determines “which role spoke what” becomes crucial.

An approach to RD is to infer roles directly from ASR transcripts [5–7]. For this, large language models (LLMs) have also been shown to be effective to some extent [6, 7]. However, text-only approaches struggle when transcripts lack distinguishing linguistic cues, for example around short back-and-forth utterances (“yeah,” “right”), due to speakers using similar vocabulary, or due to ASR errors. In these cases, acoustic information becomes essential for reliable separation.

Existing approaches combining acoustic and linguistic information for speaker-role diarization [8–12] fall into two categories: modular and end-to-end models. Modular systems, such as [10], use role-oriented language models for classification, refined by x-vector clustering. In [11], a BERT-based classifier is integrated with role-constrained x-vector clustering. However, these systems suffer from error propagation, which makes end-to-end models more appealing. Early works in this area employed a transducer model to perform ASR + RD by inserting role tokens at speaker turns in the training text [1], and explored a unified ASR + RD model for air traffic control conversations [12].

Integrating ASR and RD into a single model poses its own challenges. Direct multitask learning leads to ASR performance degradation [1, 13], a concern also noted for joint ASR+SD [2, 14]. To mitigate this, [14] trained the ASR and the turn-prediction transducers separately to preserve the word error rate (WER). For joint ASR + SD, [2] addressed this by freezing the ASR transducer and training an auxiliary SD transducer in sync via blank logit sharing (ASR-synchronized SD), a technique also adopted in [3] for speaker-attributed ASR.

Building on the success of ASR-synchronized SD [2], in this paper, we propose an ASR-synchronized RD model that predicts a role per every ASR-predicted word in parallel. For this, we show that speaker diarization and role diarization are fundamentally different tasks, requiring different acoustic and linguistic contexts, and propose appropriate modifications to the network architecture and the training strategy to tailor it for role prediction. The main contributions of this work are as follows.

1. We provide, to the best of our knowledge, the first analysis of the relative importance of acoustic and linguistic modalities for joint ASR+RD. While SD relies primarily on acoustic differences, the contribution of these modalities for RD, which involves simultaneous speaker differentiation and role inference, is not directly clear. Our results establish that RD relies more heavily on linguistic context than on acoustic features.
2. Based on this finding, we modify the baseline ASR-sync. SD model [2] for joint ASR+RD by explicitly injecting linguistic information into the RD network. This is achieved through (1) task-specific predictors (CNN for ASR and RNN for RD) and (2) the use of higher-layer ASR encoder features as input to the RD encoder. These modifications substantially improve R-WDER, with relative reductions of 19.23% on a private dataset (DoPaCo) and 54.5% on a public dataset (SiMeCo).
3. We further propose a simplified training strategy for the auxiliary RD transducer by replacing the blank-shared RNNT loss [2] with a simpler cross-entropy loss computed along the 1-best forced-alignment path. This not only reduces computational and memory requirements during training, but also yields additional relative R-WDER reductions of 3.2% on DoPaCo and 16% on SiMeCo.

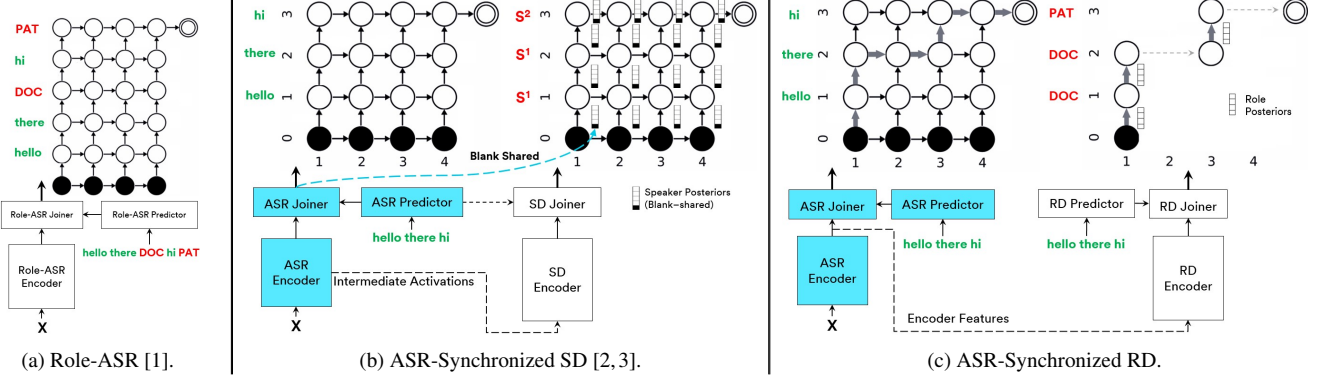


Fig. 1: Illustration of prior work in (a) and (b), along with our proposed RD training in (c), for an example audio \mathbf{x} with corresponding ground-truth label sequences: $\mathbf{y}^{\text{Role-ASR}} = [\text{hello}, \text{there}, \text{DOC}, \text{hi}, \text{PAT}]$, $\mathbf{y}^{\text{ASR}} = [\text{hello}, \text{there}, \text{hi}]$, $\mathbf{y}^{\text{SD}} = [\text{s}^1, \text{s}^1, \text{s}^2]$, and $\mathbf{y}^{\text{RD}} = [\text{DOC}, \text{DOC}, \text{PAT}]$. Blue colored ASR modules remain frozen during the training of auxiliary SD and RD transducers. The graphs at the top of each network shows the alignment paths used to compute the training loss. In (c), the path with bold arrows represent the 1-best forced-alignment path.

2. PRELIMINARIES

In this section, we revisit the Role-ASR [1] and ASR-synchronized SD [2] models that serve as baselines for this paper. Let ϕ be the blank token, $\{w^1, \dots, w^{N_{\text{ASR}}}\}$ denote the set of subwords, $\{s^1, \dots, s^{N_{\text{SD}}}\}$ the set of speakers, and $\{r^1, \dots, r^{N_{\text{RD}}}\}$ the set of speaker-roles, where $N_{\text{RD}} \leq N_{\text{SD}}$. Let a transducer model be denoted by M , where $M \in \{\text{Role-ASR}, \text{ASR}, \text{SD}, \text{RD}\}$ as shown in Figure 1. For a given audio $\mathbf{x} = [x_1, \dots, x_T]$ and the ground-truth label sequence $\mathbf{y} = [y_1, \dots, y_U]$, let the M -encoder's output be $[f_1^M(\mathbf{x}), \dots, f_T^M(\mathbf{x})]$ and the M -predictor's output be $[g_1^M, \dots, g_U^M]$, where $f_t^M \in \mathbb{R}^{N_f}$ and $g_u^M \in \mathbb{R}^{N_g}$, with t and u denoting the frame and label indices and N_f and N_g representing the encoder and predictor dimensions, respectively. Then, M -joiner's raw logits $j_{t,u}^M$ are given by

$$h_{t,u}^M = P^M \cdot f_t^M(x_{1:T}) + Q^M \cdot g_u^M(y_{1:u-1}) + b_h^M \quad (1)$$

$$j_{t,u}^M = A^M \cdot \tanh(h_{t,u}^M) + b_s^M \quad \in \mathbb{R}^{|\mathcal{V}_M|} \quad (2)$$

where P^M , Q^M and A^M are projection matrices, b_h^M and b_s^M are bias terms, and $|\mathcal{V}_M|$ is the vocabulary size. Let $\mathcal{A}(\mathbf{y})$ be the set of all possible alignments between \mathbf{y} and \mathbf{x} , more specifically between \mathbf{y} and $f_{1:T}^M(\mathbf{x})$.

2.1. Baseline 1: Role-ASR [1]

RNNT model [15] was originally proposed for ASR as an improvement over the CTC model. Shafeey et al. [1] first used it for joint ASR and RD by inserting role tokens at the end of each speaker's turn, e.g. $\mathbf{y} = [\text{hello}, \text{there}, \text{DOC}, \text{hi}, \text{PAT}]$, and training directly using the RNNT loss, as shown in Figure 1a. For this model, using Equation 1 and 2, the probability distribution over the vocabulary $\hat{y}_{t,u} \in \mathcal{V}^{\text{Role-ASR}} = \{w^1, \dots, w^{N_{\text{ASR}}}\} \cup \{r^1, \dots, r^{N_{\text{RD}}}\} \cup \{\phi\}$ is

$$\mathbb{P}(\hat{y}_{t,u} | x_{1:T}, y_{1:u-1}) = \text{softmax}(j_{t,u}^{\text{Role-ASR}}),$$

and the RNNT loss for label \mathbf{y} above is given by

$$\begin{aligned} \mathcal{L}_{\text{RNNT}} &= -\ln \mathbb{P}(\mathbf{y} | x_{1:T}) = -\ln \sum_{a \in \mathcal{A}(\mathbf{y})} \mathbb{P}(a | x_{1:T}) \\ &= -\ln \sum_{a \in \mathcal{A}(\mathbf{y})} \prod_{\hat{y}_{t,u} \in a} \mathbb{P}(\hat{y}_{t,u} | x_{1:T}, y_{1:u-1}). \end{aligned} \quad (3)$$

We use this model with an RNN predictor as our first baseline system B1: Role-ASR (RNN) in Table 2.

2.2. Baseline 2: ASR-Synchronized SD [2]

Huang et al. [2] introduced an ASR+SD model that jointly predicts words and corresponding speaker labels using two synchronized hybrid auto-regressive transducers (HAT) [16], as shown in Figure 1b. First, the ASR transducer is trained independently using the vocabulary $\mathcal{V}^{\text{ASR}} = \{w^1, \dots, w^{N_{\text{ASR}}}\} \cup \{\phi\}$. Using Equation 1 and 2, the probabilities of blank and non-blanks, $\hat{y}_{t,u} \in \mathcal{V}^{\text{ASR}}$, are given by

$$P(\hat{y}_{t,u} = \phi | x_{1:T}, y_{1:u-1}) = \text{sigmoid}(j_{t,u}^{\text{ASR}}[0]) =: b_{t,u} \quad (4)$$

$$P(\hat{y}_{t,u} = w^i | x_{1:T}, y_{1:u-1}) = (1 - b_{t,u}) \cdot \text{softmax}(j_{t,u}^{\text{ASR}}[i]),$$

for $i \in \{1, \dots, N_{\text{ASR}}\}$. Using these, the RNNT loss for an example ASR sequence $\mathbf{y} = [\text{hello}, \text{there}, \text{hi}]$ is obtained from Equation 3.

Next, the ASR transducer is frozen and the SD transducer is trained using blank-shared RNNT loss (BS-RNNT) with the vocabulary $\mathcal{V}^{\text{SD}} \cup \{\phi\}$, where $\mathcal{V}^{\text{SD}} = \{s^1, \dots, s^{N_{\text{SD}}}\}$ and ϕ is borrowed from ASR. The SD encoder takes features from an intermediate (5th) layer of the ASR encoder as input. Since SD predictor, a 1-D convolutional layer with a kernel size of 2 (CNN-2), is also borrowed from the ASR transducer, $g_u^{\text{SD}} = g_u^{\text{ASR}}$. While the blank posterior is the same as in Equation 4, the probability of speaker labels, $\hat{y}_{t,u} \in \mathcal{V}^{\text{SD}}$, are given by

$$P(\hat{y}_{t,u} | x_{1:T}, y_{1:u-1}) = (1 - b_{t,u}) \cdot \text{softmax}(j_{t,u}^{\text{SD}}).$$

Using these, the RNNT loss for a corresponding speaker-label sequence $\mathbf{y} = \{s^1, s^1, s^2\}$ is obtained from Equation 3.

During inference, whenever ASR emits $\hat{y}_{t,u} \neq \phi$, the corresponding speaker label is predicted by applying an $\text{argmax}(\cdot)$ over the SD logits $j_{t,u}^{\text{SD}}$. We apply this model as it is to RD to obtain our second baseline B2: ASR (CNN-2) + RD (CNN-2, L5) BS-RNNT in Table 2.

3. PROPOSED ASR-SYNCHRONIZED RD

In this section, we propose modifications to the ASR-Synchronized SD model in terms of (1) predictor network, (2) ASR encoder's features as input to RD encoder, and (3) training criterion to make it suitable for ASR-Synchronized RD. The rationales for these proposals are as follows.

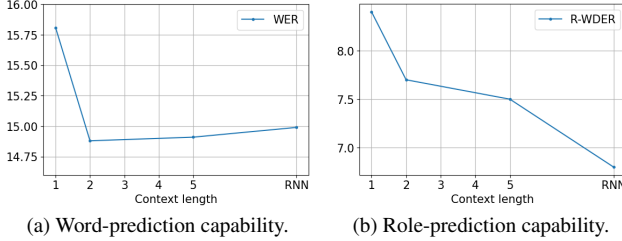


Fig. 2: Effect of Role-ASR predictor’s context length on (a) WER and (b) R-WDER when trained on DoPaCo and evaluated on the validation set of DoPaCo.

3.1. Role Diarization Relies More on Linguistic Features

Intuitively, SD is expected to rely primarily on speaker-specific acoustic cues rather than linguistic context. In contrast, RD involves not only differentiating between speakers, but also determining the roles they play in the interaction, which necessitates both acoustic and semantic (i.e., what was spoken) information. The relative importance of these two modalities, however, is not immediately clear for RD. In the following, through two complementary studies, we demonstrate that RD is more strongly influenced by linguistic context than by acoustic features.

One source of linguistic context in a transducer model is the predictor network. Using the Role-ASR model (Section 2.1), we show that while ASR may benefit from a smaller predictor’s context [16–18], role prediction definitely requires a longer context. For this, in Figure 2, we plot the word-prediction capability (WER) and the role-prediction capability (R-WDER defined in Section 4.4) of the Role-ASR model versus the predictor’s context length. To model a finite context length of n , we use CNN- n , and for an infinite context, we use an RNN. We observe that while WER remains mostly unchanged (CNN-2 being the best), R-WDER improves significantly as we increase the context length. This confirms that, unlike word prediction, role prediction benefits from the long-range linguistic information provided by the predictor. Therefore, the proposed system P1 differs from baseline system B2 by using separate task-specific predictors: CNN-2 for ASR and RNN for RD. We label this system as P1: ASR (CNN-2) + RD (RNN, L5) BS-RNNT in Table 2.

The second source of linguistic information is the word-level features from the upper layers of the ASR encoder. We show that while speaker prediction works best with features from intermediate layers (5th layer in [2]) that encode more speaker-level information, role prediction works best with features from upper layers that store more word-level information. For this, we take system P1 from above and use it with features from different layers of the ASR encoder. In Table 1, we see that R-WDER improves as we go from lower to higher layers for both the DoPaCo and SiMeCo sets. Note that since the model has been trained only on DoPaCo, R-WDER on out-of-domain SiMeCo is comparatively much worse; however, the trend is the same. Based on this, we modify the system P1 to instead use the last layer (L12) features and denote it as P2: ASR (CNN-2) + RD (RNN, L12) BS-RNNT in Table 2.

3.2. 1-Best Alignment Path + Cross Entropy Loss

The baseline system B2 [2] employs blank-factorized HAT transducers [16] so that the ASR transducer’s blank-emission probability, at each (t, u) step, can be shared with the auxiliary transducer, providing a kind of soft alignment information along all RNNT paths (Figure 1b). The auxiliary transducer then uses the full RNNT loss

ASR Enc. Layer	DoPaCo Val	SiMeCo Val
L-2	8.1	42.1
L-5	7.2	40.3
L-8	6.9	34.3
L-10	7.0	30.9
L-12	6.9	29.5

Table 1: R-WDER performance of the model ASR (CNN-2) + RD (RNN, L- n) BS-RNNT, with RD encoder taking input from different layers (L- n) of the ASR encoder. The model is trained on DoPaCo and evaluated on DoPaCo and out-of-domain SiMeCo.

(computation over all alignment paths) to train its corresponding emissions.

For our proposed method, we consider only the 1-best alignment path and train the RD-transducer simply using cross-entropy loss. For this, as shown in Figure 1c, the reference text is first forced aligned with the ASR-transducer to identify the (t, u) steps at which non-blank tokens are emitted. Then, using the cross-entropy loss, the RD network is trained to emit role tokens at its corresponding (t, u) steps. For example, for the ASR label sequence $\mathbf{y} = [\text{hello}, \text{there}, \text{hi}]$, let $\mathbf{a}^* = [\text{hello}, \text{there}, \phi, \phi, \text{hi}, \phi] \in \mathcal{A}(\mathbf{y})$ be the 1-best forced-aligned path, and $\mathbf{a}_r^* = [\text{DOC}, \text{DOC}, -, -, \text{PAT}, -]$ be the corresponding role label path (Figure 1c), where $-$ indicates no training on blank emissions. Then, with the vocabulary $\mathcal{V}^{\text{RD}} = \{1, \dots, \bar{r}^{\text{RD}}\}$, the role probabilities, for $r_{t,u} \in \mathcal{V}^{\text{RD}}$, and the cross-entropy-based RD loss are given, respectively, by

$$P(r_{t,u} | x_{1:T}, y_{1:u-1}) = \text{softmax}(j_{t,u}^{\text{RD}}),$$

$$\mathcal{L}_{\text{RD}} = \sum_{r_{t,u} \in \mathbf{a}_r^*, r_{t,u} \neq -} -\ln P(r_{t,u} | x_{1:T}, y_{1:u-1}).$$

During inference, similar to [2], at (t, u) steps where ASR emit non-blank tokens, we apply $\text{argmax}(\cdot)$ on the RD logits $j_{t, \text{speaker}, u}^{\text{RD}}$ to predict the corresponding speaker role.

Using this training method, our final proposed model P3: ASR (CNN-2) + RD (RNN, L12) 1Best-CE, in Table 2, outperforms the system trained with blank-shared (soft) alignment + RNNT loss. Unlike the RNNT loss that is computed over multiple possible alignment sequences, the 1-best alignment provides a deterministic target sequence, simplifying the optimization landscape and reducing the computational and memory overhead associated with marginalizing over the alignment matrix. This enables larger batch sizes and overall shorter training time. Moreover, while RNNT loss must be recomputed for all training samples at every epoch, forced alignments can be computed once and reused across subsequent epochs, further improving efficiency.

4. EXPERIMENTS

4.1. Dataset

For our experiments, we use an internal dataset of real-world doctor-patient conversations (DoPaCo) and a public dataset of simulated medical conversations (SiMeCo) [19].

DoPaCo consists of conversations recorded with microphones placed at medium-to-far-field positions within medical exam rooms, covering a wide range of medical specialties. These are manually transcribed and anonymized, where speakers in a conversation are labeled according to their functional role: doctor, patient, other1, other2, etc. The dataset is divided into training (1750h), validation (26.5h), and test (35.0h) sets.

SiMeCo consists of simulated near-field conversations between only two roles: doctor and patient. Of the total 272 recordings, we

Table 2: WER and R-WDER performance of different baseline and proposed models trained on DoPaCo and evaluated on DoPaCo and out-of-domain SiMeCo. The column with “finetuned” refers to DoPaCo-trained models further finetuned on SiMeCo and evaluated on SiMeCo. The type of the predictor and the ASR encoder layer from which RD encoder takes features as input are shown in parentheses. The best results are shown in bold. Since systems B2, P1, P2, and P3 share the same frozen ASR module, the WER is reported only once.

	Model	Model Size	DoPaCo Eval		SiMeCo Eval		SiMeCo Eval (finetuned)	
			WER	RWDER	WER	RWDER	WER	RWDER
Baseline	B1: Role-ASR (RNN) [1]	104M	16.03	6.5	10.62	34.2	8.8	2.2
	ASR (CNN-2) +	62.4M +	15.67	-	10.56	-	8.8	-
	B2: RD (CNN-2, L5) BS-RNNT Loss [2]	41.6M=104M	”	7.8	”	44.3	”	5.5
Ours	P1: RD (RNN, L5) BS-RNNT Loss	42.6M=105M	”	7.1	”	41.3	”	5.0
	P2: RD (RNN, L12) BS-RNNT Loss	42.6M=105M	”	6.3	”	28.9	”	2.5
	P3: RD (RNN, L12) 1Best-CE Loss	42.6M=105M	”	6.1	”	27.2	”	2.1

remove 9 that appear to be telephony. The remaining 263 conversations are from the specialties of respiratory (207), musculoskeletal (46), cardiology (5) and gastroenterology (5). Each specialty is split in a 60:20:20 ratio to form training (21.3h), validation (6.75h), and evaluation (8.5h) sets, respectively.

On all recordings, we apply a TDNN-LSTM-based voice activity detector to split them into segments of length typically less than 18 sec. For text tokenization, we use SentencePiece [20], in unigram mode [21], with a vocabulary of size 5000.

4.2. Model Architecture

The ASR encoder contains two convolutional subsampling layers that reduce the frame rate by a factor of 4, followed by 12 e-branchformer layers [22], each with a dimensionality of 384, 6-headed self-attention, and feedforward projection sublayers with 1536 dimensions. The RD encoder is similar to ASR encoder but with 9 e-branchformer layers and convolutional layers replaced by linear layers to preserve the frame rate. The RNN predictor is a single-layer LSTM with 384 dimensions, and the CNN-2 predictor is a 1-D convolutional layer with a kernel size of 2. Role-ASR transducer is made up of a 21-layer e-branchformer encoder and a 2-layer RNN predictor to match the size of the dual-transducer systems. The joint network of all transducers has 512 hidden dimensions.

4.3. Training

Models are trained using the ESPnet framework [23] using up to 20 sec long audio segments processed into 64-dim log-Mel features with speed perturbation [24] and SpecAugment [25] applied.

We train the Role-ASR and ASR transducers on DoPaCo for 40 epochs using Adam optimizer with an initial learning rate of 2×10^{-3} , warm-up scheduler with 15k warm-up steps, and a weight decay of 10^{-6} . For SiMeCo, because of its small size, we initialize the Role-ASR and ASR transducers with their corresponding DoPaCo-trained weights and then fine-tune them for 30 epochs with an initial learning rate of 10^{-4} , warm-up scheduler with 10k warm-up steps, and a weight decay of 10^{-6} . We average the ten best models based on the validation loss to get the final model.

For both DoPaCo and SiMeCo, we train the RD transducer from scratch for 30 epochs, with an initial learning rate of 10^{-4} , warm-up scheduler with 1k warm-up steps, and a weight decay of 10^{-6} . We average the ten best models based on the validation R-WDER to get the final model.

4.4. Inference and Scoring

For ASR and Role-ASR, we use beam search [15] with a beam of size 20. For RD, we follow the argmax method in Section 3.

For scoring, we use *asclite* from the NIST Scoring Toolkit (SCKT) [26] that accounts for multi-speaker alignments. The ASR

performance is measured using WER and role prediction performance is measured using role-based WDER (R-WDER). R-WDER is computed similarly to WDER [1] but words hypothesized to be spoken by the doctor can only be scored as correct against reference doctor words; same for the patient. Other-role words can match words from any single other reference speaker.

4.5. Results

In Table 2, we have the baseline models B1 and B2 as described in Section 2.1 and Section 2.2, respectively. When trained on DoPaCo and evaluated on in-domain DoPaCo, we see that ASR (CNN-2) achieves the better WER (15.67 vs. 16.03) while Role-ASR (RNN) achieves the better R-WDER (6.5 vs. 7.8). When evaluated on out-of-domain SiMeCo, we observe the effect of domain mismatch with both models performing poorly, especially in terms of R-WDER (34.2 and 44.3). When these DoPaCo-trained models are further finetuned on SiMeCo, we see the expected improvements, with both achieving the same WER (8.8) and Role-ASR again outperforming in terms of R-WDER (2.2 vs. 5.5).

The reason for the poor R-WDER performance of baseline B2, as discussed in Section 3.1, is the lack of injection of the necessary linguistic information into the RD network. Thus, applying the proposed modifications of (1) task-specific RNN predictor and (2) use of ASR encoder’s 12th-layer features, we get systems P1 and P2, respectively, that achieve significant R-WDER improvements across all settings (7.8→6.3, 44.3→28.9, 5.5→2.5). Finally, applying the 1-best alignment + cross-entropy loss, proposed in Section 3.2, we get our final system P3 that achieves the best R-WDER in all cases.

Overall, the results show that the joint ASR+RD model, with separate task-specific predictors and trained only on the 1-best forced-aligned ASR path using cross-entropy loss, outperforms the baseline models in terms of both WER and R-WDER.

5. CONCLUSION

This work demonstrated that a modified version of the auxiliary speaker diarization network [2] can be successfully adapted for speaker-role diarization, achieving superior performance over the integrated approach in [1]. The study also established that, unlike speaker prediction, role prediction depends more on linguistic context than on acoustic cues, motivating two modifications: (1) separate task-specific predictors: CNN for ASR and an RNN for role prediction, and (2) the use of higher-layer ASR encoder features which encode richer linguistic information. In addition, replacing the RNNT loss with a cross-entropy loss along the 1-best forced-alignment path simplified the training of the role prediction network and significantly improved performance. Future work will explore training strategies leveraging the middle ground of n -best paths.

6. REFERENCES

- [1] Laurent El Shafey, Hagen Soltau, and Izhak Shafran, “Joint speech recognition and speaker diarization via sequence transduction,” in *Interspeech 2019*, 2019, pp. 396–400.
- [2] Yiling Huang, Weiran Wang, Guanlong Zhao, Hank Liao, Wei Xia, and Quan Wang, “On the success and limitations of auxiliary network based word-level end-to-end neural speaker diarization,” in *Interspeech 2024*, 2024, pp. 32–36.
- [3] Desh Raj, Matthew Wiesner, Matthew Maciejewski, Paola Garcia, Daniel Povey, and Sanjeev Khudanpur, “On speaker attribution with surt,” in *The Speaker and Language Recognition Workshop (Odyssey 2024)*, 2024, pp. 91–98.
- [4] Federico Landini, Ján Profant, Mireia Diez, and Lukáš Burget, “Bayesian hmm clustering of x-vector sequences (vbx) in speaker diarization: Theory, implementation and analysis on standard tasks,” *Computer Speech & Language*, 2022.
- [5] Juan Zuluaga-Gomez, Seyyed Saeed Sarfjoo, Amrutha Prasad, Iuliia Nigmatulina, Petr Motlicek, Karel Ondrej, Oliver Ohneiser, and Hartmut Helmke, “Bertraffic: Bert-based joint speaker role and speaker change detection for air traffic control communications,” in *Proc. IEEE SLT*, 2023.
- [6] Quan Wang, Yiling Huang, Guanlong Zhao, Evan Clark, Wei Xia, and Hank Liao, “DiarizationLM: Speaker Diarization Post-Processing with Large Language Models,” *arXiv preprint arXiv:2401.03506*, 2024.
- [7] Peilin Wu and Jinho D Choi, “Do we still need audio? re-thinking speaker diarization with a text-based approach using multiple prediction models,” *arXiv e-prints*, pp. arXiv–2506, 2025.
- [8] Fabio Valente, Deepu Vijayasan, and Petr Motlicek, “Speaker diarization of meetings based on speaker role n-gram models,” in *Proc. IEEE ICASSP*, 2011.
- [9] Ashtosh Sapru, Sree Harsha Yella, and Hervé Bourlard, “Improving speaker diarization using social role information,” in *2014 IEEE ICASSP*, 2014.
- [10] Nikolaos Flemotimos, Panayiotis Georgiou, and Shrikanth Narayanan, “Linguistically aided speaker diarization using speaker role information,” in *The Speaker and Language Recognition Workshop (Odyssey 2020)*. ISCA, 2020.
- [11] Nikolaos Flemotimos and Shrikanth Narayanan, “Multimodal Clustering with Role Induced Constraints for Speaker Diarization,” in *Proc. Interspeech*, 2022.
- [12] Alexander Blatt, Aravind Krishnan, and Dietrich Klakow, “Joint vs Sequential Speaker-Role Detection and Automatic Speech Recognition for Air-traffic Control,” in *Proc. Interspeech*, 2024.
- [13] Bongjun Kim, Arindam Ghosh, Mark C. Fuhs, Anurag Chowdhury, Deblin Bagchi, and Monika Woszcyna, “A Hybrid Approach to Combining Role Diarization with ASR for Professional Conversations,” in *Interspeech 2025*, 2025, pp. 5243–5247.
- [14] Shuo-Yiin Chang, Bo Li, Tara Sainath, Chao Zhang, Trevor Strohman, Qiao Liang, and Yanzhang He, “Turn-taking prediction for natural conversational speech,” in *Interspeech 2022*, 2022, pp. 1821–1825.
- [15] Alex Graves, “Sequence transduction with recurrent neural networks,” *arXiv preprint arXiv:1211.3711*, 2012.
- [16] Ehsan Variani, David Rybach, Cyril Allauzen, and Michael Riley, “Hybrid autoregressive transducer (hat),” in *ICASSP 2020 - 2020 IEEE International Conference on Acoustics, Speech and Signal Processing (ICASSP)*, 2020, pp. 6139–6143.
- [17] Mohammadreza Ghodsi, Xiaofeng Liu, James Apfel, Rodrigo Cabrera, and Eugene Weinstein, “Rnn-transducer with stateless prediction network,” in *ICASSP 2020 - 2020 IEEE International Conference on Acoustics, Speech and Signal Processing (ICASSP)*, 2020, pp. 7049–7053.
- [18] Rohit Prabhavalkar, Yanzhang He, David Rybach, Sean Campbell, Arun Narayanan, Trevor Strohman, and Tara N. Sainath, “Less is more: Improved rnn-t decoding using limited label context and path merging,” in *ICASSP 2021 - 2021 IEEE International Conference on Acoustics, Speech and Signal Processing (ICASSP)*, 2021, pp. 5659–5663.
- [19] Faiha Fareez, Tishya Parikh, Christopher Wavell, Saba Shabbab, Meghan Chevalier, Scott Good, Isabella De Blasi, Rafik Rhouma, Christopher McMahon, Jean-Paul Lam, Thomas Lo, and Christopher W. Smith, “A dataset of simulated patient-physician medical interviews with a focus on respiratory cases,” *Scientific Data*, vol. 9, 2022.
- [20] Taku Kudo and John Richardson, “SentencePiece: A simple and language independent subword tokenizer and detokenizer for neural text processing,” in *Proceedings of the 2018 Conference on Empirical Methods in Natural Language Processing: System Demonstrations*, Eduardo Blanco and Wei Lu, Eds., Brussels, Belgium, Nov. 2018, pp. 66–71, Association for Computational Linguistics.
- [21] Taku Kudo, “Subword regularization: Improving neural network translation models with multiple subword candidates,” in *Proceedings of the 56th Annual Meeting of the Association for Computational Linguistics (Volume 1: Long Papers)*, Iryna Gurevych and Yusuke Miyao, Eds., Melbourne, Australia, July 2018, pp. 66–75, Association for Computational Linguistics.
- [22] Kwangyoun Kim, Felix Wu, Yifan Peng, Jing Pan, Prashant Sridhar, Kyu J. Han, and Shinji Watanabe, “E-branchformer: Branchformer with enhanced merging for speech recognition,” in *2022 IEEE Spoken Language Technology Workshop (SLT)*, 2023.
- [23] Shinji Watanabe, Takaaki Hori, Shigeki Karita, Tomoki Hayashi, Jiro Nishitoba, Yuya Unno, Nelson Enrique Yalta Sopplin, Jahn Heymann, Matthew Wiesner, Nanxin Chen, Adithya Renduchintala, and Tsubasa Ochiai, “ESPnet: End-to-end speech processing toolkit,” in *Proceedings of Interspeech*, 2018, pp. 2207–2211.
- [24] Tom Ko, Vijayaditya Peddinti, Daniel Povey, and Sanjeev Khudanpur, “Audio augmentation for speech recognition,” in *Interspeech 2015*, 2015, pp. 3586–3589.
- [25] Daniel S. Park, William Chan, Yu Zhang, Chung-Cheng Chiu, Barret Zoph, Ekin D. Cubuk, and Quoc V. Le, “SpecAugment: A simple data augmentation method for automatic speech recognition,” in *Interspeech 2019*, 2019, pp. 2613–2617.
- [26] NIST, “SCTK, the NIST Scoring Toolkit,” <https://github.com/usnistgov/SCTK>, 2021.

Appendix

A. SPEAKER-ROLE DIARIZATION GUIDED ASR DECODING

In this section, we show how feedback from auxiliary RD transducer can be used to improve ASR decoding. Unlike [2, 3], where the ASR transducer is untouched to avoid interference from the auxiliary task, we use the RD posteriors to propose a blank-suppression heuristic that can reduce deletion errors.

As shown in Table 3, the ASR transducer with a CNN-2 predictor experiences high deletion errors on DoPaCo. A potential solution to recover these deletions, without modifying the model, is to suppress the incorrect blanks and promote the deleted correct word tokens during the beam search. However, the challenge remains: how do we identify the (t, u) -steps in the beam search where blank suppression is needed?

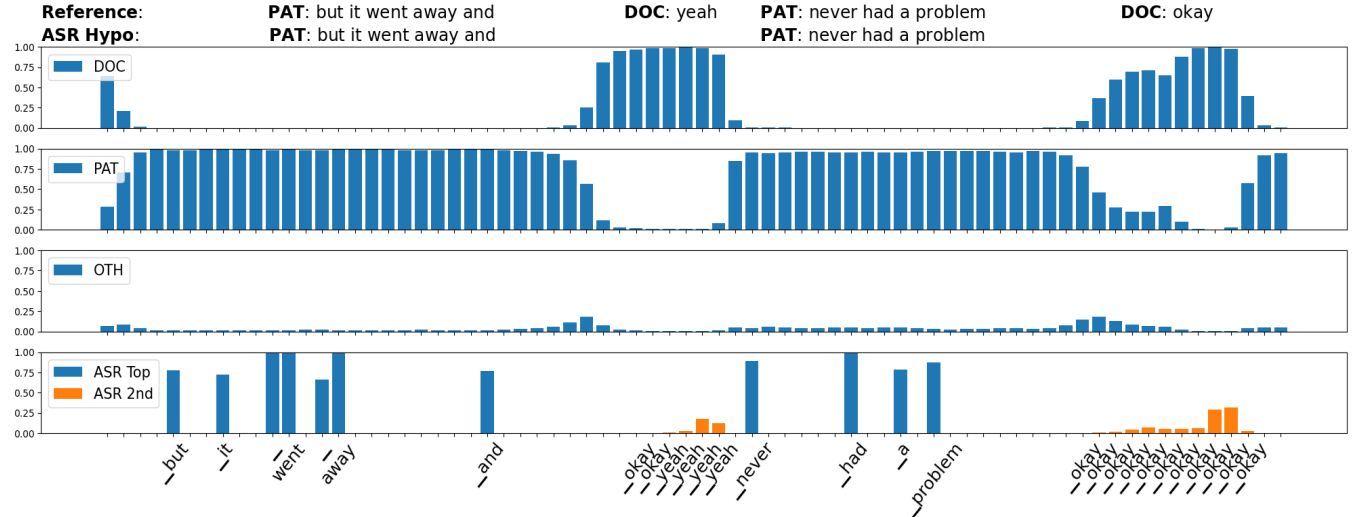


Fig. 3: Activity of ASR and RD networks at each (t, u) -step of the best beam search path. The reference and hypothesis are shown at the top. The top three plots show the RD network's posteriors for DOC, PAT, and OTH. The bottom-most plot shows the ASR posteriors for the top token in blue (blank token omitted to avoid clutter) and the second-best token (for two specific regions) in orange.

For this, in Figure 3, we plot the posterior activity of our ASR (CNN-2) + RD (RNN) model for the utterance “PAT: but it went away and; DOC: yeah; PAT: never had a problem; DOC: okay”. The bottom-most plot shows that ASR deletes “yeah” and “okay” spoken by DOC, as blank is the most likely token in those regions. The top three plots reveal that although the RD network is trained only on frames where a subword token is emitted, its activity at other frames indicates an awareness of speaker activity. Notably, the RD network correctly detects DOC’s activity (top-most plot) in the deleted regions. If we plot the second-best ASR tokens (orange in the bottom-most plot), we find that they are indeed “yeah” and “okay”, suggesting that RD activity can provide valuable signals for blank suppression.

Based on this, we propose a blank-suppression heuristic, outlined in Algorithm 1, wherein we first identify the set of top- n deleted tokens D_n from the validation set. Then, at any (t, u) -step of the ASR beam search, where the top non-blank token has a sufficiently high posterior ($\geq \alpha$) and belongs to D_n , and the RD network confidently ($\geq \beta$) detects role activity, we transfer the probability mass from blank to non-blank tokens. For DoPaCo, we tune the parameters using the validation set, setting $\alpha = 0.1$, $\beta = 0.99$, and $D_n = \{\text{yeah}, \text{okay}\}$. Additionally, to prevent excessive insertions, we enforce a minimum gap of three steps between consecutive suppressions.

Algorithm 1 RD-Guided ASR Blank Suppression

- ```

1: Set α, β, D_n (set of top- n deleted tokens from val set).
2: for every (t, u) -step along a beam search path do
3: $p_{t,u}^{\text{ASR}} = \text{softmax}(j_{t,u-1}^{\text{ASR}})$
4: $p_{t,u}^{\text{RD}} = \text{softmax}(j_{t,u-1}^{\text{RD}})$
5: if $\text{argmax}(p_{t,u,1:N_{\text{ASR}}}^{\text{ASR}}) \in D_n \wedge \max(p_{t,u,1:N_{\text{ASR}}}^{\text{ASR}}) \geq \alpha \wedge \max(p_{t,u}^{\text{RD}}) \geq \beta$ then
6: $p_{t,u,\phi}^{\text{ASR}} = 0.01$ # Set it to some low value
7: $p_{t,u}^{\text{ASR}} = p_{t,u}^{\text{ASR}} / \sum_v p_{t,u,v}^{\text{ASR}}$
8: end if
9: end for

```

We find that applying the heuristic to all tokens does not yield any overall improvement because while this helps to reduce deletions for some tokens, it also increases the insertions. Too much rise in insertions will eventually nullify the improvement due to reduction in deletions. Thus, we first use the val set to identify the tokens that have the most deletions and then selectively apply our blank-suppression to them. In

order to do so, in Figure 4, we plot the WER versus  $n \in \{1, \dots, 10\}$ , where top- $n$  deletion tokens are applied blank suppression. We find that the most benefit we get from RD-guided decoding is when we apply it only top-2 deletion tokens.

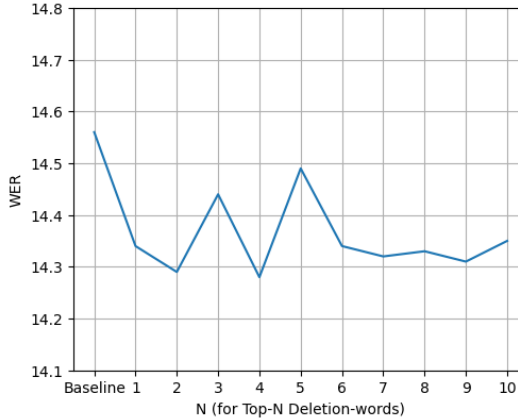


**Fig. 4:** DoPaCo validation set: reduction in WER when top- $n$  ( $n \in [1, 2, \dots, 10]$ ) deletion-words are accounted for during RD-guided ASR decoding. The top-10 deletion-words for the validation set are: yeah, okay, I, and, it, you, a, the, oh, right.

In Table 3, we see that the ASR (CNN-2) + RD (RNN) model has disproportionately high deletions compared to insertions. To reduce them, we apply our proposed blank suppression heuristic in Algorithm 1 and see that it improves the WER of the frozen ASR on both val and eval sets ( $14.56 \rightarrow 14.29$ ,  $15.67 \rightarrow 15.65$ ). From Table 3, we further see that RD-guided decoding is successful in doing its intended job of reducing deletion errors ( $6.47 \rightarrow 6.33$ ,  $6.69 \rightarrow 6.60$ ). However, in the eval set, due to an unwanted increase in insertions ( $1.74 \rightarrow 1.80$ ), the improvement is a bit muted. The reason could be that since the RD capability of ASR (CNN-2) + RD (RNN) on the eval set is slightly weaker to begin with, the RD network's guidance provides only a marginal benefit.

**Table 3:** Substitution, deletion, and insertion errors of ASR (CNN-2) + RD (RNN) model with different decoding strategies.

|      | ASR (CNN-2) + RD (RNN) | WER   | SUB  | DEL  | INS  |
|------|------------------------|-------|------|------|------|
| Val  | Beam Search            | 14.56 | 6.36 | 6.47 | 1.73 |
|      | RD-Guided Beam Search  | 14.29 | 6.38 | 6.33 | 1.58 |
| Eval | Beam Search            | 15.67 | 7.24 | 6.69 | 1.74 |
|      | RD-Guided Beam Search  | 15.65 | 7.25 | 6.60 | 1.80 |

Although RD-guided blank suppression yields only marginal improvements on the evaluation set, the approach nonetheless shows clear promise. While the RD network is trained only on frames where ASR subword tokens are emitted, its activity on other frames indicates an implicit awareness of speaker activity across the entire audio. We demonstrated that this insight can help reduce small-word deletions, and future work will further investigate how to better address the suppressed-word phenomenon identified in this study.